

# UC Berkeley

## UC Berkeley Previously Published Works

### Title

Connecting primordial gravitational waves and dark energy

### Permalink

<https://escholarship.org/uc/item/04c7n5b2>

### Journal

Journal of Cosmology and Astroparticle Physics, 2023(09)

### ISSN

1475-7516

### Authors

Zhumabek, Tilek  
Denissenya, Mikhail  
Linder, Eric V

### Publication Date

2023-09-01

### DOI

10.1088/1475-7516/2023/09/013

### Copyright Information

This work is made available under the terms of a Creative Commons Attribution License, available at <https://creativecommons.org/licenses/by/4.0/>

Peer reviewed

# Connecting Primordial Gravitational Waves and Dark Energy

Tilek Zhumabek<sup>1,2</sup>, Mikhail Denissenya<sup>1</sup>, Eric V. Linder<sup>1,3</sup>

<sup>1</sup>*Energetic Cosmos Laboratory, Nazarbayev University, Astana 010000, Qazaqstan*

<sup>2</sup>*Department of Physics, School of Sciences and Humanities,  
Nazarbayev University, Astana 010000, Qazaqstan*

<sup>3</sup>*Berkeley Center for Cosmological Physics & Berkeley Lab,  
University of California, Berkeley, CA 94720, USA*

(Dated: September 12, 2023)

Cosmic acceleration manifested in the early universe as inflation, generating primordial gravitational waves detectable in the cosmic microwave background (CMB) radiation. Cosmic acceleration is occurring again at present as dark energy, detectable in cosmic distance and structure surveys. We explore the intriguing idea of connecting the two occurrences through quintessential inflation by an  $\alpha$ -attractor potential without a cosmological constant. For this model we demonstrate robustness of the connection  $1 + w_0 \approx 4/(3N^2 r)$  between the present day dark energy equation of state parameter  $w_0$  and the primordial tensor to scalar ratio  $r$  for a wide range of initial conditions. Analytic and numerical solutions produce current thawing behavior, resulting in a tight relation  $w_a \approx -1.53(1 + w_0) \approx -0.2(4 \times 10^{-3}/r)$ . Upcoming CMB and galaxy redshift surveys can test this consistency condition. Within this model, lack of detection of a dark energy deviation from  $\Lambda$  predicts a higher  $r$ , and lack of detection of  $r$  predicts greater dark energy dynamics.

## I. INTRODUCTION

Inflation and dark energy govern two major epochs of cosmic history and drastically change the universe. Inflation, through quantum fluctuations, generates structure from the vacuum, creating both matter and radiation density perturbations and tensor perturbations of space-time itself, that are primordial gravitational waves. Dark energy has come to dominate the cosmic energy density recently, leading to rapid expansion of distances and suppression of the growth of cosmic structure that occurred during the matter dominated epoch.

While accelerated expansion is in common between the two eras, they are separated by billions of year in time, or some 60 e-folds in expansion. Thus the idea of unifying their mechanisms, known as quintessential inflation (see, e.g., [1–8]), is both attractive and problematic. If they arise from the dynamics of a scalar field rolling on its potential, the potential itself is difficult to rationalize and the difference in energy scales (roughly  $10^{25}$  eV for inflation,  $10^{-3}$  eV for dark energy) is large. The hierarchy problem is well known and is a general puzzle even if we ascribe dark energy simply to a cosmological constant [9]. However ideas from supergravity present a robust concept for the inflation potential through  $\alpha$ -attractors [10–12]. As well  $\alpha$ -attractors can be employed for dark energy, e.g. [13, 14]. Finally, the unification of the two as quintessential inflation has been considered, e.g. [6, 15–21].

We explore  $\alpha$ -attractors, which includes Starobinsky gravity, as quintessential inflation in more detail, demonstrating and highlighting the important characteristic that they behave as thawing scalar fields. This helps motivate the large gap in time between the two episodes of cosmic acceleration. The field rolled along its plateau during inflation, ending when the potential steepened and the energy density diminished, but Hubble friction

governed the dynamics, freezing the field until recently when the field was released to thaw and gradually deviate from its cosmological constant-like torpor. Thawing fields have specific characteristics that can be derived analytically, and the equations of motion can be evaluated numerically to check.

The remarkable aspect of quintessential inflation combined with the  $\alpha$ -attractor formalism is that predictions from the two eras are tightly connected, moreover in an “everybody wins something” manner. If the tensor to scalar ratio  $r$  of perturbation power generated by inflation is low (making it difficult for future CMB experiments to detect), i.e. the potential is too flat, then it freezes higher up its potential and has more dynamics once it thaws in the dark energy phase. Conversely, if  $r$  is large enough for easier detection due to the potential being steeper then the field traverses further and thaws recently in a flatter part of the potential, giving less dark energy dynamics. We explore which wins under what circumstances, and whether there is a happy medium where both experimental signals are accessible. We work with a potential with no cosmological constant, i.e. zero minimum, so that all the cosmic acceleration is from the  $\alpha$ -attractor dynamics, and that none was “put in by hand”.

Section II provides a brief summary of  $\alpha$ -attractors and sets up the coupled system of equations of motion. In Section III we solve the dynamics, demonstrating the dependence of results on physics inputs such as  $\alpha$  and the frozen field value. We demonstrate in Section IV both analytically and numerically that viable results belong to the thawing class of dark energy and have definite relations between  $r$  and the dark energy equation of state parameters  $w_0$  and  $w_a$ . Section V discusses constraints from future CMB and cosmic distance and structure experiments, with results from each guiding the other. We discuss and summarize our results in Section VI.

## II. $\alpha$ -ATTRACTORS AS QUINTESSENTIAL INFLATION

The class of  $\alpha$ -attractor models has several attractive features, including high energy physics and symmetry motivations; see [10–12] for details. These involve a Lagrangian density with a scalar field with a pole kinetic term and a potential,

$$\mathcal{L} = \frac{1}{2}R - \frac{1}{2} \frac{(\partial\phi)^2}{\left(1 - \frac{\phi^2}{6\alpha}\right)^2} - V\left(\frac{\phi}{\sqrt{6\alpha}}\right) + \mathcal{L}_m, \quad (1)$$

where  $\mathcal{L}_m$  is the matter Lagrangian and we set the reduced Planck mass  $M_P = 8\pi G = 1$  (so  $\phi$  is dimensionless). The field has poles at  $\phi = \pm\sqrt{6\alpha}$ . The parameter  $\alpha$  controls the position of the pole [22], and can also be interpreted geometrically in taking discrete values related to the symmetry class [23, 24].

Due to the behavior near the pole, the field rolls very slowly, allowing for a high energy inflationary epoch. Quite generically this leads to predictions for the inflationary curvature perturbation power spectrum tilt  $n_s$  and the tensor to scalar perturbation power ratio  $r$ ,

$$n_s = 1 - \frac{2}{N}, \quad r = \frac{12\alpha}{N^2}, \quad (2)$$

where  $N$  is the number of e-folds between horizon crossing and the end of inflation, generally of order 50–60. The Poincaré disk scenario of  $\alpha$ -attractors gives discrete values of  $3\alpha = 1, 2, \dots, 7$ , while Starobinsky and Higgs inflation models possess  $\alpha = 1$ .

Specific details of the inflationary evolution will depend on the potential chosen. It is convenient to use a canonically normalized field  $\varphi$  instead of the original field  $\phi$  through the transformation

$$\phi = \sqrt{6\alpha} \tanh \frac{\varphi}{\sqrt{6\alpha}}. \quad (3)$$

This moves the poles to  $\varphi = \pm\infty$  and explicitly demonstrates the inflationary plateau where the field rolls slowly. The potential  $V(\varphi)$  generally rolls off the plateau at large  $\varphi$  with an exponential deviation, due to the tanh function.

We are particularly interested in quintessential inflation  $\alpha$ -attractor models, where after inflation the field rolls to much smaller values (by  $\sim 10^{110}$ ) of the potential energy suitable for late time dark energy cosmic acceleration. One way of achieving late time acceleration is including a cosmological constant  $\Lambda$  in the potential, i.e. another plateau at energy scale  $\Lambda$ . We do not take this approach, but rather seek a dynamical dark energy with zero cosmological constant. Furthermore, just as there is attractor behavior at early times regarding the observables  $n_s$  and  $r$ , we want to avoid fine tuning by using a potential with attractor behavior at late times, of an exponential potential form.

These desiderata are satisfied by the potential,

$$V(\phi) = M^2 e^{-2g} \left[ e^{g\left(\frac{\phi}{\sqrt{6\alpha}} + 1\right)} - 1 \right] \quad (4)$$

$$V(\varphi) = M^2 e^{-2g} \left[ e^{g(\tanh(\varphi/\sqrt{6\alpha}) + 1)} - 1 \right], \quad (5)$$

called by [17] as Exp-model II; we call it the ExpLin model since  $V(\phi)$  approaches the positive pole as an exponential (giving inflation) and the negative pole as a linear function in  $\phi + \sqrt{6\alpha}$  (which translates to an exponential in  $\varphi$ ; note the linear potential, in addition to the pole structure, gives some protection against quantum corrections for this dark energy part of the potential). Here  $M^2$  gives the inflation energy scale and  $M^2 e^{-2g}$  will be of order the current dark energy density (hence  $g \approx 125$ ; while still not of order one, the exponential relaxes the huge hierarchy).

Since the dark energy part of the potential has an exponential form,

$$V(\varphi \rightarrow -\infty) \approx M^2 e^{-2g} 2g e^{-2|\varphi|/\sqrt{6\alpha}}, \quad (6)$$

i.e.  $V \sim e^{-\lambda\varphi}$ , then we will have an attractor behavior to  $w_\infty = -1 + \lambda^2/3 = -1 + 2/(9\alpha)$ . Thus we have the very nice relation that

$$1 + w_\infty = \frac{8}{3N^2 r} = 0.22 \left(\frac{51}{N}\right)^2 \left(\frac{4.6 \times 10^{-3}}{r}\right). \quad (7)$$

(The parameter values used for illustration correspond to the simple Starobinsky model as given in [25].) That is, if  $r$  is so small as to evade detection in CMB polarization B-modes, we stand a good chance of seeing a signature in late time acceleration different from a cosmological constant ( $w = -1$ ), while if there is no deviation from a cosmological constant observed then this predicts (within this quintessential inflation model) that inflationary gravitational waves should be detected at a reasonable value of  $r$ .

We solve the exact dynamics of the quintessential inflation field through numerical evaluation of its equation of motion, the Klein-Gordon equation, plus the Friedmann equation. We implement this as an autonomous system of coupled ordinary differential equations (see, e.g., [26]) for the kinetic and potential energies, using variables  $x = \varphi'/\sqrt{6}$ ,  $y = \sqrt{V(\varphi)/(3H^2)}$ :

$$x' = -3x + \sqrt{\frac{3}{2}} \lambda y^2 + \frac{3}{2} x [2x^2 + \gamma(1 - x^2 - y^2)] \quad (8)$$

$$y' = -\sqrt{\frac{3}{2}} \lambda y x + \frac{3}{2} y [2x^2 + \gamma(1 - x^2 - y^2)]. \quad (9)$$

Here  $H$  is the Hubble parameter and a prime denotes a derivative with respect to the e-fold time variable  $\ln a$ . The background equation of state parameter  $\gamma$  (neglecting the field) and the fractional potential slope  $\lambda$  are

$$\gamma = 1 + \frac{1}{3} \frac{1}{1 + \frac{\Omega_m}{\Omega_r} e^{\ln a}} \quad (10)$$

$$\lambda = -\frac{V_{,\varphi}}{V}, \quad (11)$$

where  $\Omega_m$  and  $\Omega_r$  are the present fractions of energy density in matter and radiation, respectively, relative to the critical density.

To test the numerical accuracy we have also implemented the coupled equations in the three equation form [26], defining  $\Gamma = VV_{,\varphi\varphi}/V_{,\varphi}^2$  and including the evolution equation

$$\lambda' = -\sqrt{6}\lambda^2(\Gamma - 1)x. \quad (12)$$

The results are identical to desired precision, and we use the two equation system for all results presented.

### III. DYNAMICAL RESULTS

The field evolution is determined by the model parameter  $\alpha$ , and the initial conditions on the field,  $\varphi_i = \varphi_f$  i.e. the frozen value. Note though that we expect the attractor behavior to give evolution substantially independent of  $\varphi_f$  over some range. We set initial conditions at  $\ln a = -15$  ( $z \approx 3 \times 10^6$ ). Due to the high Hubble friction at early times, results are independent of  $\varphi'_i$ , and we set it to zero as appropriate for the frozen field state. The matter density today will affect late time results and our fiducial value is  $\Omega_m = 0.3$  (and where necessary we adopt  $H_0 = 68$  km/s/Mpc). We generally consider a range of  $\alpha = [1/3, 7/3]$ , to match the values corresponding to the Poincaré disk  $\alpha$ -attractor origin.

Figure 1 shows the field evolution as a function of  $\alpha$  and of  $\varphi_f$ . As expected, the field is frozen during the matter dominated epoch and only rolls at close to the present ( $\ln a = 0$ ). Such behavior is known as a thawing field [13, 27, 28] and will have important physical consequences discussed in Sec. IV. The smaller  $\alpha$ , the steeper the potential and the sooner and more vigorously it thaws (see the left panel). Also, the closer  $\varphi_f$  is to zero, the steeper the potential (i.e. the further from the  $\varphi \rightarrow -\infty$  approach to  $V = 0$ ) and again the field thaws sooner and more strongly (see the right panel).

The dark energy dynamics can be usefully described through the equation of state parameter, or pressure to density ratio,  $w(a)$ . Figure 2 illustrates the evolutionary behavior. While the field is frozen,  $w = -1$ , and then as it thaws it moves away from cosmological constant behavior and becomes less negative. In the future it goes to its attractor behavior  $w_\infty = -1 + 2/(9\alpha)$ . Depending on the steepness of the potential it may overshoot and then relax to the attractor. Note that for  $\varphi_f \lesssim -15$  the equation of state is rather insensitive to  $\varphi_f$ , while for  $\varphi_f \gtrsim -10$  the deviation near the present is so extreme that it will be severely constrained by observations.

### IV. RELATIONS BETWEEN INFLATION AND DARK ENERGY

As we have seen, the ExpLin  $\alpha$ -attractor model has a definite relation between the inflationary tensor to scalar

ratio  $r$  and the late time attractor dark energy equation of state parameter  $w_\infty$ . However, late time observations do not constrain  $w_\infty$  directly but rather cosmic distances and growth factors that involve  $w(a)$ . Therefore we need to examine how  $w(a)$  behaves.

The form  $w(a) = w_0 + w_a(1-a)$  has been demonstrated [29, 30] to be an excellent fit to observations (distances and growth factors) relative to the exact equation of motion, to  $\sim 0.1\%$  accuracy, especially for thawing fields. Therefore we investigate the relation of the parameters  $w_0$  and  $w_a$  to the model parameters.

First, we connect  $w_\infty(\alpha)$  to  $w_0$ . Figure 2 already hints that there is a close connection for viable models, i.e. those that do not overshoot the attractor to larger  $w$ . We quantify the ratio  $P \equiv (1 + w_0)/(1 + w_\infty)$  in Figure 3. Indeed we find that over the range of  $\alpha$  under consideration, and for viable  $\varphi_f$ , we have

$$1 + w_0 \approx 0.5(1 + w_\infty), \quad (13)$$

to a good approximation. Thus we can relate inflationary  $r$  to dark energy  $w_0$ , so Eq. (7) becomes

$$1 + w_0 \approx \frac{4}{3N^2r} = 0.10 \left(\frac{51}{N}\right)^2 \left(\frac{4.6 \times 10^{-3}}{r}\right). \quad (14)$$

As for the time variation of the dark energy equation of state parametrized by  $w_a$ , we recall that many thawing fields have a narrow relation  $w_a \approx -(1 + w_0) \times (1.5 - 1.6)$  as demonstrated in [30]. To investigate whether that holds for ExpLin we solve numerically the coupled equations of motion; note that  $w(a) = (x^2 - y^2)/(x^2 + y^2)$ . The parameter  $w_0$  is simply  $w(a = 1)$ , while Ref. [30] established that  $w_a$  has a physical interpretation as a calibration, or stretching, parameter to unify members of a particular class (i.e. parameter values within a model). From the phase space quantity  $w'$  we can define  $w_a = -w'(a)/a$  and evaluate it at some  $a = a_*$  as described in [30]. This only affects the theory *interpretation* – bringing members of a theory family close together – and not the observables that treat  $w_0$  and  $w_a$  as fit parameters within  $w(a) = w_0 + w_a(1 - a)$ . Following Ref. [30], we seek to select  $a_*$  by where the phase space evolution  $w-w'$  has a nearly universal track for different model parameters.

Figure 4 demonstrates the calibration by computing  $Q \equiv w_a/(1 + w_0)$  as a function of  $a_*$ . We see that most of the models lie close to each other for a broad range of  $a_*$ , and lie within the standard thawing behavior. Both for variation of  $\alpha$  (roughly  $\alpha \gtrsim 2/3$ : we can see from the left panel of Fig. 2 that  $\alpha = 1/3$  has a quite strong deviation from  $w = -1$  and is not viable observationally) and  $\varphi_f$  over its viable range the value  $a_* \approx 0.65$  (i.e.  $z \approx 0.5$ ) gives an especially tight calibration, i.e.

$$w_a \approx -1.53(1 + w_0). \quad (15)$$

Thus we can also rewrite the relation Eq. (14) between inflation and dark energy as

$$w_a \approx \frac{-6}{3N^2r} = -0.16 \left(\frac{51}{N}\right)^2 \left(\frac{4.6 \times 10^{-3}}{r}\right). \quad (16)$$

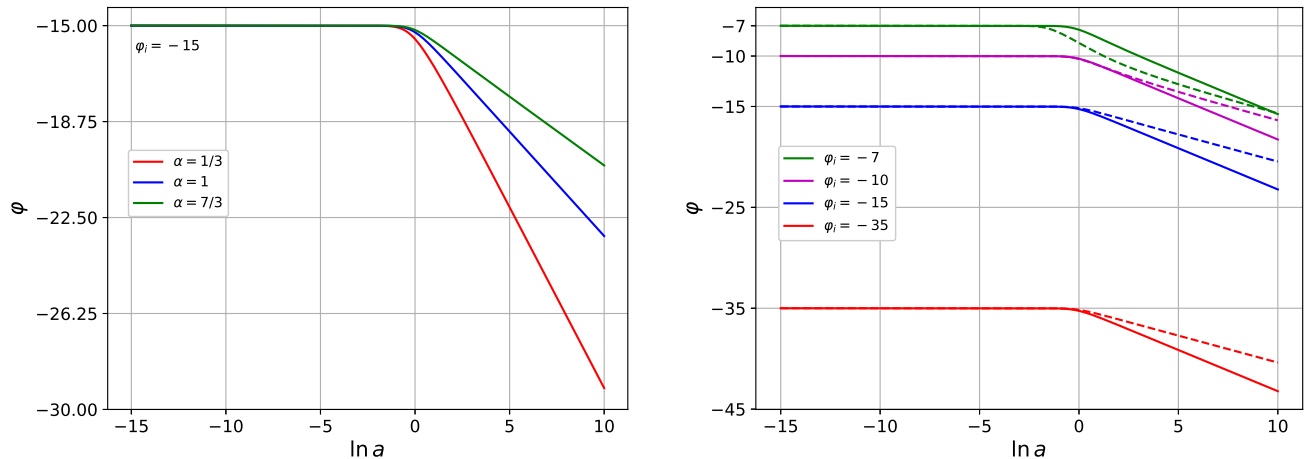


FIG. 1. The field thaws from the frozen state induced by high Hubble friction, and rolls down the potential with a rapidity determined by its steepness. [Left panel] We illustrate the dependence on  $\alpha$ , fixing  $\varphi_i \equiv \varphi_f = -15$ . [Right panel] We illustrate the dependence on  $\varphi_f$ , fixing  $\alpha = 1$  (solid curves) or  $\alpha = 7/3$  (dashed curves).

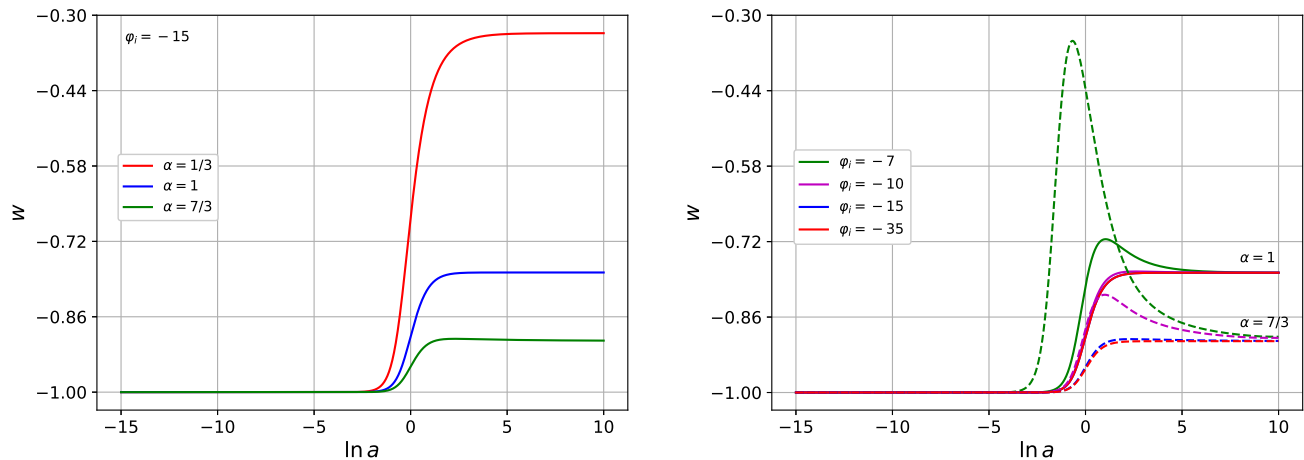


FIG. 2. The dark energy equation of state parameter  $w(a)$  evolves from a cosmological constant state to its future attractor value. [Left panel] The smaller  $\alpha$  and hence the steeper the potential, the sooner and more that  $w(a)$  deviates from  $-1$ . Values  $\alpha < 1$  will have difficulty being consistent with observations. [Right panel] The less negative  $\varphi_f$  is and hence the steeper the potential, the sooner and more that  $w(a)$  deviates from  $-1$ . Note that very steep potentials can cause  $w$  to overshoot its attractor value. Values  $\varphi_f > -10$  will have difficulty being consistent with observations, while values  $\varphi_f < -15$  give near identical results.

To verify and illustrate the relations among  $w_0$ - $w_a$ - $r$  we show the exact solutions for these quantities over a range of  $\alpha$  and  $\phi_i$ . Figure 5 shows where the models lie in the  $w_0$ - $w_a$  space, with colors corresponding to different  $\alpha$  and symbols to different  $\phi_i$ . They lie tightly clustered along the relation of Eq. (15), showing that  $w_a$  is indeed a dynamical physics calibration parameter. Slight deviations start to arise only outside the viable region,  $w_0 > -0.8$  (see Section V). All models depend little on  $\varphi_f$  for  $\varphi_f \lesssim -10$ , and even out to  $\varphi_f \approx -8$  stay on the  $w_0$ - $w_a$  relation; those that deviate at  $\varphi_f > -8$  again tend to lie in the unviable regime.

Figure 6 demonstrates the correspondence between in-

flationary  $r$  and the dark energy parameters. For a given  $\alpha$  the derived values for  $r$ ,  $w_0$ ,  $w_a$  are plotted, using  $\varphi_f = -15$  (but we just saw that  $w_0$  and  $w_a$  are rather insensitive to  $\varphi_f$  over the viable range). The tensor to scalar ratio  $r$  in Eq. (2) scales as  $1/N^2$  for fixed  $\alpha$  (while dark energy dynamics does not depend on  $N$ , thawing from a late time frozen state), and we show a band from  $N = [50, 60]$  (this band should cover a reasonable range of inflation reheating scenarios), with the solid curve linking the different  $\alpha$  values for  $N = 51$ . We explicitly see that dark energy dynamics and the strength of the primordial gravitational wave signature are inversely proportional, so that within this model if we fail to detect

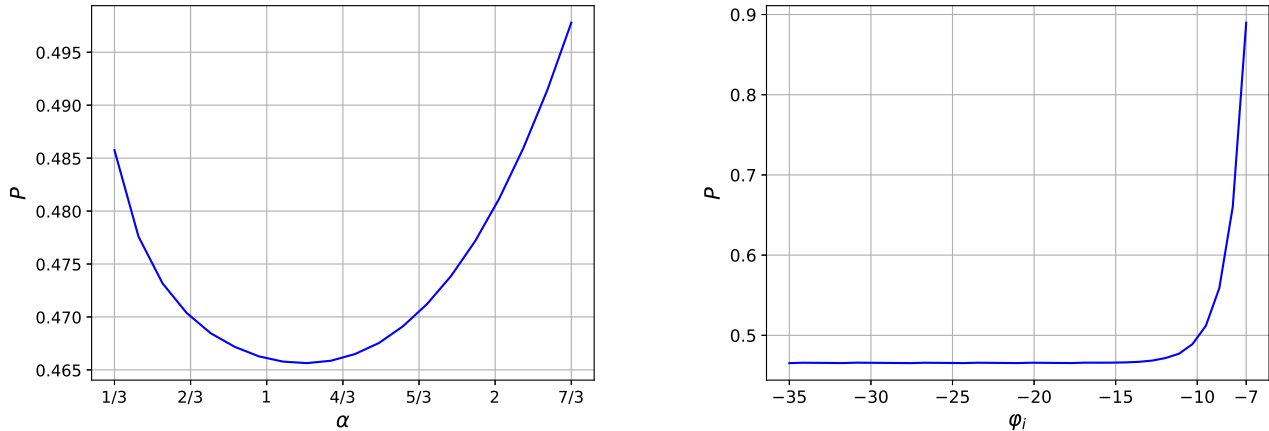


FIG. 3. The ratio  $P \equiv (1 + w_0)/(1 + w_\infty)$  is nearly constant over the range of  $\alpha$  (left panel, with  $\varphi_f = -15$ ) and viable  $\varphi_f$  (right panel, with  $\alpha = 1$ ) considered.

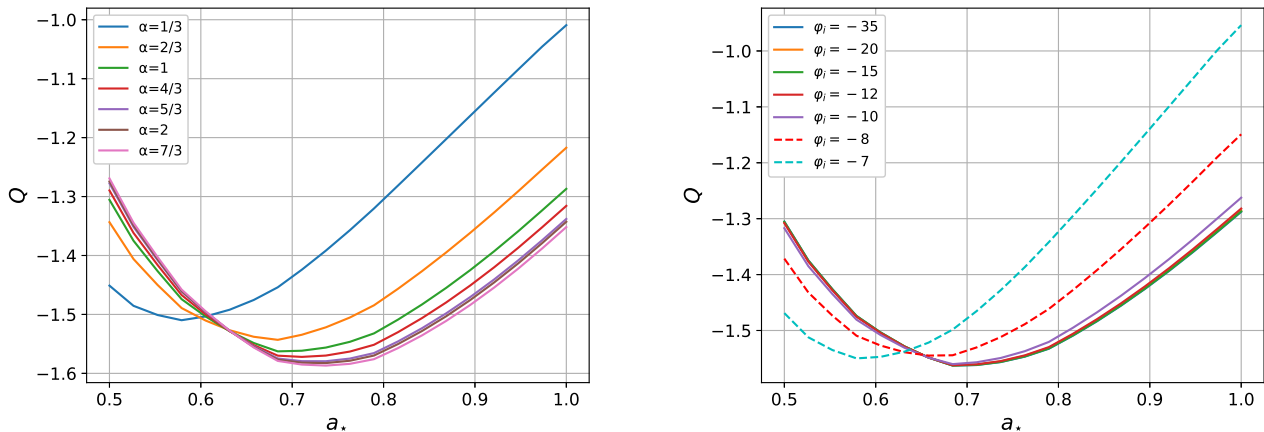


FIG. 4. The ratio  $Q \equiv w_a/(1 + w_0)$ , with  $w_a = -w'(a_*)/a_*$ , shows that the ExpLin model acts like a standard thawing field and is well calibrated (nearly universal phase space behavior – curves at nearly the same value) for  $a_* \approx 0.65$  over the viable parameter range. [Left panel] Variation with respect to  $\alpha$ , for  $\varphi_f = -15$ ; [Right panel] Variation with respect to  $\varphi_f$ , for  $\alpha = 1$ .

primordial gravitational waves we are likely to see dark energy dynamics distinct from a cosmological constant, while conversely if we fail to detect dark energy dynamics we are likely to detect primordial gravitational waves. With next generation experiments in both the CMB and cosmic distance/structure surveys, we may well detect both as measurement uncertainties should be of order (e.g. [31–34])  $\sigma(r) \approx 5 \times 10^{-4}$ ,  $\sigma(w_0) \approx 0.08$ ,  $\sigma(w_a) \approx 0.2$  (while there are plans for experiments to improve these further).

## V. CONSTRAINTS FROM OBSERVATIONS

We can connect the quintessential inflation parameters to observables through fairly simple relations. First, from

Eq. (2) we have

$$N = \frac{2}{1 - n_s} = 57 \frac{1 - 0.965}{1 - n_s} \quad (17)$$

$$\alpha = \frac{r}{3(1 - n_s)^2} = 1.24 \frac{r}{4.6 \times 10^{-3}} \left( \frac{1 - 0.965}{1 - n_s} \right)^2 \quad (18)$$

where  $n_s$  and  $r$  are observable from the CMB.

The mass scale  $M$  of the potential can be related to the amplitude of observed CMB temperature perturbations  $A_s$  arising from inflation by (see, e.g., [17])

$$M^2 = \frac{144\pi^2\alpha N}{(2N - 3\alpha)^3} A_s \approx 10^{-10} \alpha. \quad (19)$$

Finally the exponential potential index  $g$  comes from the late time dark energy epoch (see Eq. 6) by making sure

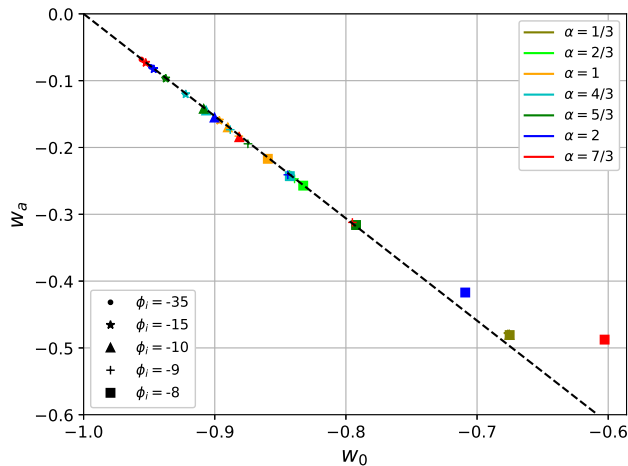


FIG. 5. Numerical solutions for dark energy equation of state parameters, denoted by colors and symbols corresponding to different  $\alpha$  and  $\varphi_f$ , are in good agreement with Eq. (15) shown by the dashed line. Only outside of the viable region do deviations start to appear (note  $\alpha = 1/3$  has all symbols on top of each other).

the fractional dark energy today takes a value  $\Omega_{\text{de},0} = 1 - \Omega_m$  as desired. The parameter  $g$  can efficiently be found for a particular value, e.g.  $\Omega_{\text{de},0} = 0.7$ , by bisection. Results for  $g$  ( $\approx 120$ – $128$ ) as a function of  $M^2$  and  $\varphi_f$  are shown in the top right panel of Fig. 15 of [17] (note they write  $\gamma$  instead of  $g$  and  $\varphi_F$  instead of  $\varphi_f$ ).

In the previous section we have demonstrated the tight relations between  $w_0$  and  $w_\infty = -1 + 2/(9\alpha)$ ,  $w_0$  and  $w_a$ , and hence  $r$  and  $w_0, w_a$ . While  $w_0$  and  $w_a$  will eventually be determined by observations involving distances and the growth of cosmic structure (along with  $r$  from CMB B-mode polarization, giving a strong consistency test), we already have bounds on dark energy indicating that its dynamics does not vary too much from cosmological constant behavior. For example, the reduced distance to CMB last scattering for  $w_0 = -0.8$  (and hence also with  $w_a \approx -0.3$  by the thawing relation) differs from the LCDM prediction by 1.1%, well above the Planck constraints [35]. One would have to shift  $\Omega_m$  by 0.02 between the  $(w_0, w_a) = (-0.8, -0.3)$  model – giving a distance corresponding roughly to a constant  $w = -0.9$  model – and LCDM to move within the 0.4% distance constraint. Thus we consider models more extreme,  $w_0 > -0.8$ , to be disfavored.

Since a strong connection exists between inflationary gravitational waves and dark energy dynamics in this model, then an experiment seeing a signature for one

can inform the other type of experiment on the desired sensitivity level, i.e. “where to look”. Furthermore, the thawing nature of the dark energy field raises the probative power of experiments that have good leverage on the dynamics in terms of  $w_a$ , as well as the recent universe value  $w_0$ .

## VI. CONCLUSIONS

We are on the cusp of experiments that will probe the early (inflation) and late (dark energy) epochs of cosmic acceleration with unprecedented accuracy. Lack of a signal of primordial gravitational waves and of dynamics distinct from a cosmological constant would give limited insight into the physics behind these fundamental phenomena. Quintessential inflation however ties these epochs together, and  $\alpha$ -attractors provide some definite predictions. The  $\alpha$ -attractor ExpLin model considered here has some important characteristics in terms of simple functions, symmetry protection against some quantum corrections, and avoidance of some fine tuning.

The plateau with exponential potential part for inflation and the linear potential part (translating to an exponential potential free of a cosmological constant in the canonical field) for dark energy leads to tight relations between the inflation and dark energy observables. Late time acceleration arises out of a thawing field with a calibrated relation  $w_a = -1.53(1 + w_0)$  and dynamics leading to an attractor giving  $1 + w_0 \approx 0.5(1 + w_\infty)$ . Since  $w_\infty$  is tied to the model parameter  $\alpha$ , as is the inflation tensor-to-scalar ratio  $r$ , this predicts strong connections between all the observables. We have verified this numerically and illustrated the insensitivity to initial conditions over a broad range.

In a “can’t lose” manner, values of  $\alpha$  near the higher end of the fundamental physics predicted range will give a primordial gravitational wave signal, while those near the lower end will give a dark energy dynamics signal. The values near the middle of the range, e.g. Starobinsky inflation’s  $\alpha = 1$ , will give signals in both that should be accessible to next generation experiments – an exciting prospect!

## ACKNOWLEDGMENTS

This work was supported in part by the Energetic Cosmos Laboratory. EL is supported in part by the U.S. Department of Energy, Office of Science, Office of High Energy Physics, under contract number DE-AC02-05CH11231.

[1] P. J. E. Peebles and A. Vilenkin, Quintessential inflation, *Phys. Rev. D* **59**, 063505 (1999), [arXiv:astro-ph/9810509](https://arxiv.org/abs/astro-ph/9810509).

[2] C. Baccigalupi and F. Perrotta, Perturbations in quintessential inflation, (1998), [arXiv:astro-ph/9811385](https://arxiv.org/abs/astro-ph/9811385).

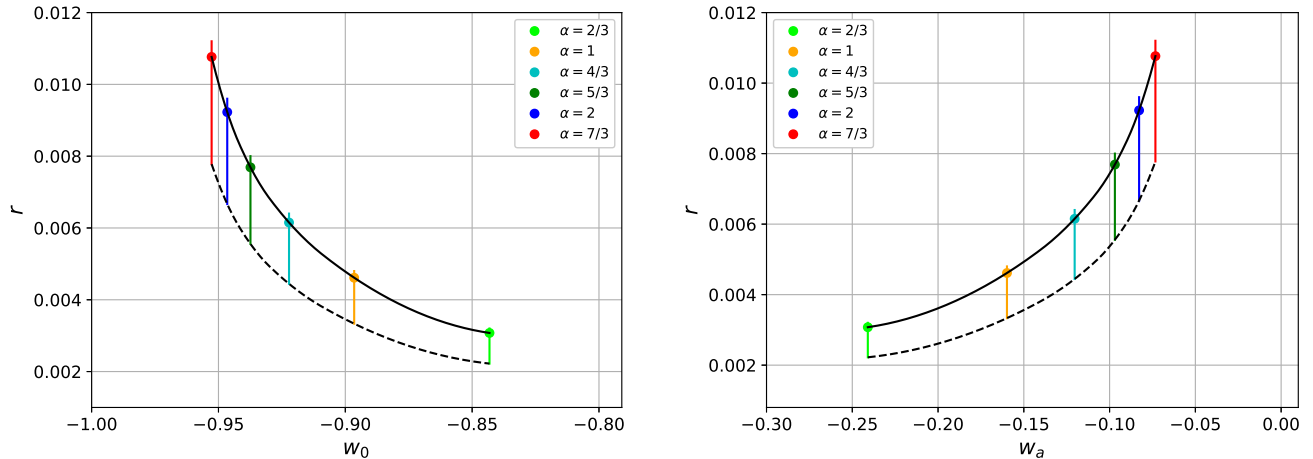


FIG. 6. The connection between the strength of inflationary gravitational waves, given by  $r$ , and the dark energy dynamics, given by  $w_0$  (left panel) or  $w_a$  (right panel), is tight as shown by the curves (here for  $\varphi_f = -15$  but nearly the same over its viable range). Solid (dashed) black curves link the different  $\alpha$  values for  $N = 51$  (60), with vertical colored lines running over  $N = [50, 60]$  for constant  $\alpha$ .

- [3] K. Dimopoulos and J. W. F. Valle, Modeling quintessential inflation, *Astropart. Phys.* **18**, 287 (2002), [arXiv:astro-ph/0111417](#).
- [4] R. Rosenfeld and J. A. Frieman, A Simple model for quintessential inflation, *JCAP* **09**, 003, [arXiv:astro-ph/0504191](#).
- [5] M. Wali Hossain, R. Myrzakulov, M. Sami, and E. N. Saridakis, Unification of inflation and dark energy à la quintessential inflation, *Int. J. Mod. Phys. D* **24**, 1530014 (2015), [arXiv:1410.6100 \[gr-qc\]](#).
- [6] K. Dimopoulos, Jointly modelling Cosmic Inflation and Dark Energy, *J. Phys. Conf. Ser.* **2105**, 012001 (2021), [arXiv:2106.14966 \[gr-qc\]](#).
- [7] J. de Haro and L. A. Saló, A Review of Quintessential Inflation, *Galaxies* **9**, 73 (2021), [arXiv:2108.11144 \[gr-qc\]](#).
- [8] D. Bettoni and J. Rubio, Quintessential Inflation: A Tale of Emergent and Broken Symmetries, *Galaxies* **10**, 22 (2022), [arXiv:2112.11948 \[astro-ph.CO\]](#).
- [9] S. Weinberg, The Cosmological Constant Problem, *Rev. Mod. Phys.* **61**, 1 (1989).
- [10] R. Kallosh and A. Linde, Universality Class in Conformal Inflation, *JCAP* **07**, 002, [arXiv:1306.5220 \[hep-th\]](#).
- [11] R. Kallosh, A. Linde, and D. Roest, Superconformal Inflationary  $\alpha$ -Attractors, *JHEP* **11**, 198, [arXiv:1311.0472 \[hep-th\]](#).
- [12] M. Galante, R. Kallosh, A. Linde, and D. Roest, Unity of Cosmological Inflation Attractors, *Phys. Rev. Lett.* **114**, 141302 (2015), [arXiv:1412.3797 \[hep-th\]](#).
- [13] E. V. Linder, Dark energy from  $\alpha$ -attractors, *Physical Review D* **91**, 10.1103/physrevd.91.123012 (2015), [arXiv:1505.00815 \[astro-ph.CO\]](#).
- [14] M. Braglia, W. T. Emond, F. Finelli, A. E. Gümrükçüoğlu, and K. Koyama, Unified framework for early dark energy from  $\alpha$ -attractors, *Physical Review D* **102**, 10.1103/physrevd.102.083513 (2020), [arXiv:2005.14053 \[astro-ph.CO\]](#).
- [15] K. Dimopoulos and C. Owen, Quintessential Inflation with  $\alpha$ -attractors, *JCAP* **06**, 027, [arXiv:1703.00305 \[gr-qc\]](#).
- [16] K. Dimopoulos, L. Donaldson Wood, and C. Owen, Instant preheating in quintessential inflation with  $\alpha$ -attractors, *Phys. Rev. D* **97**, 063525 (2018), [arXiv:1712.01760 \[astro-ph.CO\]](#).
- [17] Y. Akrami, R. Kallosh, A. Linde, and V. Vardanyan, Dark energy,  $\alpha$ -attractors, and large-scale structure surveys, *Journal of Cosmology and Astroparticle Physics* **2018** (06), 041, [arXiv:1803.00661 \[astro-ph.CO\]](#).
- [18] C. García-García, E. V. Linder, P. Ruíz-Lapuente, and M. Zumalacárregui, Dark energy from  $\alpha$ -attractors: phenomenology and observational constraints, *JCAP* **08**, 022, [arXiv:1803.00661 \[astro-ph.CO\]](#).
- [19] Y. Akrami, S. Casas, S. Deng, and V. Vardanyan, Quintessential  $\alpha$ -attractor inflation: forecasts for stage IV galaxy surveys, *Journal of Cosmology and Astroparticle Physics* **2021** (04), 006, [arXiv:2103.07892 \[astro-ph.CO\]](#).
- [20] L. Aresté Saló, D. Benisty, E. I. Guendelman, and J. de Haro,  $\alpha$ -attractors in quintessential inflation motivated by supergravity, *Phys. Rev. D* **103**, 123535 (2021), [arXiv:2103.07892 \[astro-ph.CO\]](#).
- [21] W. Giarè, S. Pan, E. Di Valentino, W. Yang, J. de Haro, and A. Melchiorri, Inflationary Potential as seen from Different Angles: Model Compatibility from Multiple CMB Missions, (2023), [arXiv:2305.15378 \[astro-ph.CO\]](#).
- [22] R. Kallosh, A. Linde, and D. Roest, Large field inflation and double  $\alpha$ -attractors, *JHEP* **08**, 052, [arXiv:1405.3646 \[hep-th\]](#).
- [23] S. Ferrara and R. Kallosh, Seven-disk manifold,  $\alpha$ -attractors, and  $B$  modes, *Phys. Rev. D* **94**, 126015 (2016), [arXiv:1610.04163 \[hep-th\]](#).
- [24] R. Kallosh, A. Linde, T. Wrase, and Y. Yamada, Maximal Supersymmetry and B-Mode Targets, *JHEP* **04**, 144, [arXiv:1704.04829 \[hep-th\]](#).
- [25] E. Allys *et al.* (LiteBIRD), Probing Cosmic Inflation with the LiteBIRD Cosmic Microwave Background



- Polarization Survey, *PTEP* **2023**, 042F01 (2023), [arXiv:2202.02773 \[astro-ph.IM\]](#).
- [26] E. J. Copeland, M. Sami, and S. Tsujikawa, Dynamics of dark energy, *International Journal of Modern Physics D* **15**, 1753 (2006), [arXiv:hep-th/0603057](#).
- [27] R. R. Caldwell and E. V. Linder, Limits of quintessence, *Physical Review Letters* **95**, [10.1103/physrevlett.95.141301](#) (2005), [arXiv:astro-ph/0505494](#).
- [28] E. V. Linder, Paths of quintessence, *Physical Review D* **73**, [10.1103/physrevd.73.063010](#) (2006), [arXiv:astro-ph/0601052](#).
- [29] E. V. Linder, Exploring the expansion history of the universe, *Physical Review Letters* **90**, [10.1103/physrevlett.90.091301](#) (2003), [arXiv:astro-ph/0208512](#).
- [30] R. de Putter and E. V. Linder, Calibrating dark energy, *Journal of Cosmology and Astroparticle Physics* **2008** (10), 042, [arXiv:0808.0189 \[astro-ph\]](#).
- [31] A. Aghamousa *et al.* (DESI), The DESI Experiment Part I: Science, Targeting, and Survey Design, (2016), [arXiv:1611.00036 \[astro-ph.IM\]](#).
- [32] R. Mandelbaum *et al.* (LSST Dark Energy Science), The LSST Dark Energy Science Collaboration (DESC) Science Requirements Document, (2018), [arXiv:1809.01669 \[astro-ph.CO\]](#).
- [33] K. Abazajian *et al.*, CMB-S4 Science Case, Reference Design, and Project Plan, (2019), [arXiv:1907.04473 \[astro-ph.IM\]](#).
- [34] A. Blanchard *et al.* (Euclid), Euclid preparation: VII. Forecast validation for Euclid cosmological probes, *Astron. Astrophys.* **642**, A191 (2020), [arXiv:1910.09273 \[astro-ph.CO\]](#).
- [35] N. Aghanim *et al.* (Planck), Planck 2018 results. VI. Cosmological parameters, *Astron. Astrophys.* **641**, A6 (2020), [arXiv:1807.06209 \[astro-ph.CO\]](#).